



Cite this: *Nanoscale Adv.*, 2022, **4**, 2806

Hydrophobic soot nanoparticles as a non-cytotoxic motility activator of human spermatozoa[†]

Karekin D. Esmeryan, ^{*a} Ivaylo Rangelov ^b and Todor A. Chaushev^b

Sperm cryopreservation is vital in combating the human infertility, but regrettably, the toxicity of cryoprotectants and the occurrence of intracellular icing, osmotic shocks or shrinkage of the cells below a given threshold volume greatly affects the success rate of this technique. Using the virtue of nanotechnologies and depositing water-repellent soot nanoparticles on the inner walls of cryovials may outline new directions in the development of cryobiology, but doubts related to the soot's venomosity question its practical implementability. The scientific content of this article eliminates the existing apprehensions by analyzing the cytotoxicity of three types of rapeseed oil soot, differing in morphology, surface chemistry and zeta potential, towards human spermatozoa. Upon intermittent evaluations of the sperm motility within 270 min of incubation in vials comprising carbon nanoparticles, we reveal that this soot category is non-cytotoxic or at worst, faintly toxic to the gametes provided by twenty individuals. Enhanced progressive sperm motility is observed at ~50–60% of patients following the soot treatments, which is attributed to electrostatic repulsions and biochemical alterations in the seminal plasma. These fascinating results open new horizons for incorporation of the rapeseed oil soot as a tool for functional preparation and activation of human spermatozoa preceding *in vitro* fertilization.

Received 29th March 2022
Accepted 22nd April 2022

DOI: 10.1039/d2na00192f
rsc.li/nanoscale-advances

1. Introduction

The prospect of overcoming death, considered as an opportunity for maintaining eternal life, has played a key role in the religious beliefs and historical development of the human civilization for millennia.¹ Hypothetically, immortality might be reached if the biochemical processes (aging) in living organisms are drastically delayed or completely terminated, which might be feasible at cryogenic temperatures.² Despite the hopes that the future medical technologies could facilitate the revival of humans undergoing full-body cryopreservation, the ethical consequences of such clinical procedures and the inevitable damage of the brain's neural networks during vitrification^{1,3} impart controversial character of the contemporary cryonics. Therefore, the natural human reproduction *via* sexual intercourses is still the preferred way of continuing the genus and transferring parental genomes in time,⁴ *i.e.*, partially approaching biological immortality.

Nowadays, the hectic lifestyle along with the exorbitant consumption of alcohol, drugs and genetically-modified foods increase male sterility, which currently encompasses ~7–12%

of the sexually active men^{5–7} with the terrifying possibility of ending up with most of the male population in USA and Europe being infertile by 2060.⁸ This worrisome tendency has provoked the emergence of assisted reproductive technologies (ART), where the sperm freezing strategies are beneficial for preserving reproductively active spermatozoa in a controllable manner.⁹ This is critical in cases of autoimmune diseases, surgical infertility interventions, vasectomy, cancer treatments, human immunodeficiency virus or hepatitis B, because the short- and long-term cryostorage of human semen provides a chance for post-treatment use of own gametes for reproduction.^{10–15}

So far, the efficiency of sperm cryoprotection techniques involving slow cooling is limited due to the formation of ice crystals, inflicting trauma and/or a lethal end to parts of the frozen material.^{16,17} In particular, the cooling velocity determines the likelihood for intracellular icing and the cells' survival rate following cryopreservation.¹⁸ The freezing injury is argued to be a consequence of the crystallization processes and increased solute concentrations when the water is replaced by ice, inducing osmotic imbalances and cell membrane rupture.^{18,19} These shortcomings can be overcome by executing “shock cooling” (vitrification) associated with impeded molecular diffusion and instant phase transition of the liquid into an amorphous solid,²⁰ which would, however, irreversibly destroy the cytoskeleton and chromatin structure of the gametes.¹⁶ The inclusion of cryoprotective agents alleviates the cryostorage of living matter by supporting supersaturation (incomplete cell freezing) and enhancing the osmotic strength.^{21,22}

^aAcoustoelectronics Laboratory, Georgi Nadjakov Institute of Solid State Physics, Bulgarian Academy of Sciences, 72, Tzarigradsko Chaussee Blvd., 1784 Sofia, Bulgaria. E-mail: karekin_esmerian@abv.bg; Tel: +359 2 979 5811

^bResearch Department, Medical Center Neovitro OOD, 20, Petko Y. Todorov Blvd., 1408 Sofia, Bulgaria

† Electronic supplementary information (ESI) available. See <https://doi.org/10.1039/d2na00192f>



Unfortunately, their toxicity at high concentrations^{23–25} imposes the cryopreservation of human spermatozoa in an artificial seminal plasma (relying on its self-protective function) without cryoprotectants²⁶ or *via* the addition of 5% high-molecular polyvinylpyrrolidone polymer,²⁷ risking the loss of sperm motility and mitochondrial activity (nearly 40–50%, according to Table S2† and Fig. 3 in ref. 26 and 27, respectively).

Higher cryotolerance of the motile spermatozoa might be achieved *via* low surface energy chemical modifications of any preliminary roughened solid (e.g., the inner walls of cryovials), converting the working interface into superhydrophobic.²⁸ The superhydrophobicity minimizes the solid–liquid contact area (even for liquid columns instead of single droplets²⁸), so the heat transfer rate and icing probability are reduced by natural means, hindering the incipiency of ice nuclei.^{29–31} Using these unique properties, Esmeryan *et al.* have demonstrated that ~80% of the initial motility of post-thawed sperm cells restores if the substrate-of-interest is coated with non-wettable soot nanoparticles.³² Further experiments have confirmed the hypothesis that an osmotic movement outwards the cell matrix is mainly responsible for the semen's uniform dehydration, similarly to the germplasm freezing,³³ because the cooling of water droplets residing on a soot-coated surface leads to simultaneous freezing of the three-phase contact line and the liquid's entire outer shell (the shell is approximated to a cell membrane), but the bulk remains slurry.³⁴ Although the International Society for Cryobiology has qualified the study as eye-opening, part of this community has claimed that it goes against the basic principles of cryobiology.³² Moreover, the European Green Deal, approved in 2020, and the aspirations for the decarbonization of the industry, aiming to gain lower output of greenhouse gases (e.g., soot emissions) in the troposphere, enforce the common perception that carbon soot is a highly hazardous substance and must remain in history.³⁵ Indeed, apart from changing the Earth's radiative balance, the atmospheric soot aerosols adversely affect the human health and often cause lung cancer or cardiovascular diseases.³⁶ From that point of view, the recently proposed soot-based approach for cryoprotection of human gametes is quite curious, unthinkable and even questionable to a certain extent.³²

The paramount objective of this research is to explore and elucidate whether the rapeseed oil-generated soot, employed as a novel platform for cryopreservation of human semen,³² renders any cytotoxicity to the sperm cells at patients with distinct seminal parameters – an issue that has not been clarified yet, but standing as a cornerstone for the eventual applicability of the aforementioned technology in fertility clinics. The new data introduced herein are essential for establishing the physico-chemical soot–spermatozoa interactions with direct relevance to the subsequent effects on sperm motility – a knowledge that is presently absent in the scientific literature.

2. Experimental procedures

2.1. Soot production

For accomplishing the cytotoxicity studies, a variety of soot nanoparticles were generated by accurately regulating the air flow rate, *via* a flow meter/controller (Fisher Scientific 11998014,

Germany), required to maintain the incomplete combustion of a rapeseed oil-impregnated wick situated in a steel conical combustion chamber – a well-known technique ensuring reproducible synthesis of extremely water-repellent soot.^{32,34,37–39} Three basic types of soot particles/aggregates with adjustably variable shape, size, surface oxidation and zeta potential, classified as *soot1* – *soot2* – *soot3*, were deposited as coatings on a series of microscope glass slides at air flow values of $0.0052\text{ m}^3\text{ min}^{-1}$, $0.0042\text{ m}^3\text{ min}^{-1}$ and $0.0033\text{ m}^3\text{ min}^{-1}$, and stored in Petri dishes.

2.2. Materials characterization

The soot specimens were characterized through scanning electron microscopy (SEM), energy dispersive spectroscopy (EDS), zeta potential and wettability analyses. High-resolution SEM images were taken with a Hitachi SU-70 field emission scanning electron microscope at magnifications of 50 kX. The chemical composition of the soot was defined *via* EDS measurements performed at 15 keV with an EDAX detector having an active area of 10 mm^2 . A plastic cuvette filled with 1.5 mL distilled water and 0.1 mg soot powder was subjected to dynamic light scattering and electrophoretic light scattering, using a Zetasizer Nano ZS Ver. 7.12 (Malvern Panalytical, UK) analytical instrument, in order to quantify the particle size and surface charge. An optical system OCA 15EC (DataPhysics, Germany) was used to determine the static contact angle (SCA) and contact angle hysteresis (CAH) on the soot as average of three independent experimental cycles with 10 μL distilled water droplets.

2.3. Human ejaculate collection and cytotoxicity analysis

Twenty patients with deteriorated seminal parameters or from couples with idiopathic infertility (refers to a medical condition in which the clinical examination does not reveal any pathological finding explaining the inability of gaining pregnancy) were selected as representatives of the male factor infertility. Their native ejaculates were collected *via* masturbation and excretion of the material into sterile containers after 24–120 h of sexual restraint. Upon liquefaction, the sperm concentration and motility were identified and recorded by means of a computer software (Sperm Class Analyzer software 6.0.0.2 Microptic S.L., Barcelona Spain). Each liquified seminal fluid was divided into three (at nine patients) or four (at eleven patients) equal aliquots and placed in plastic vials through an automatic micropipette. Then, the soot coatings (see Section 2.1) were carefully peeled off the glass slides and 1000 ppm of each soot powder type (two or three types, depending on the number of prepared aliquots) were mixed severally with the human ejaculate contained in the vials (e.g., 200 μg soot distributed in 200 μL semen), while the remaining soot-free vial was left as a control. The cell-soot suspensions were vortexed and incubated at $T \sim 37\text{ }^\circ\text{C}$ and $RH \sim 98\%$, and the kinetics of cytotoxicity (if manifested) was explored on every 90 min until more than 90% immotile spermatozoa were noticed in the control sample compared to its original (fresh) state.



The rationale of our experimental setup is related to the unanticipated sperm motility activation detected throughout the assays comprising two ultimately different classes of carbon nanoparticles, motivating us to include a third “intermediate” soot pattern. In addition, 1000 ppm of dispersed soot particulates is the highest concentration, ensuring operation of the CASA software without significant measurement errors. Signed informed consents and institutional ethical approval were obtained prior to using the ejaculates for research, in compliance with the license of Neovitro OOD for assisted reproduction activities (ref. no. 9260/10.03.2021).

3. Results and discussion

3.1. Morphology, chemistry, wettability and zeta potential of the rapeseed oil soot

The controlled combustion of vegetable oils is a well-developed method offering inexpensive, facile and one-step fabrication of non-wettable soot with exhaustively examined physicochemical characteristics.^{32,34,37–42} Therefore, the morphochemical features shown in Fig. 1 and 2 are routinely discussed and are intended to serve as a benchmark for interpreting the impact of this group of soot nanoparticles on the sperm cells' motility.

Gradually decreasing the air flow rate induces conversion of the conventional fractal-like spherical soot (Fig. 1a) into carbon clusters composed of fragmentary particles with unclear external boundaries (Fig. 1b) or completely fused quasi-square-shaped soot agglomerates with lacking interparticle borderlines (Fig. 1c), in perfect agreement with the current state-of-the-art.^{40,42} The stepwise lowering of the atmospheric air flow alters likewise the chemical kinetics of the nascent carbon nanoparticles,⁴⁰ leading to sequential reduction in the quantity of oxygen atoms occupying the soot (see Fig. 2), repeatedly observable elsewhere too.^{34,37–39} Independently of the surface morphology and chemistry, all samples are superhydrophobic and possess SCA \sim 160–164° and CAH \sim 1–2° due to their non-polarity and nanoscale roughness.^{34,37–39}

Since the human spermatozoa are negatively charged (-16 mV/ -20 mV) and their functionality correlates with the cell membrane's zeta potential,⁴³ which, on the other hand, governs the cytotoxicity of nanomaterials to different microorganisms,^{44,45} it is imperative to measure the surface charge of soot samples, as illustrated in Fig. 3.

Apparently, the weaker the surface oxidation, the higher the negative charge of the rapeseed oil soot (e.g., $1.9 \rightarrow 1.4 \rightarrow 1.1$ at% O

at% O correspond to $-23.3 \rightarrow -28.2 \rightarrow -31.3$ mV), in contrast to the increased zeta potential of the highly oxidized diesel soot.⁴⁶ However, the surface charge of TiO₂ nanoparticles, for instance, is directly proportional to their specific surface area,⁴⁷ which is believed to be the reason why the largest *soot3* agglomerates (\sim 1170 nm, based on the Zetasizer instrument's readings) are the most negatively charged solids as compared to the smaller *soot2* (\sim 530 nm) and *soot1* (\sim 180 nm) aggregates, satisfying the Smoluchowski's theory.⁴⁸

3.2. Influence of the rapeseed oil soot on sperm motility

Cardiovascular dysfunctions and respiratory diseases are among the frequently observed health complications in humans exposed to soot aerosols,³⁶ which is a basis for equitable medical concerns regarding the consequences of any soot interactions with the sperm cells during cryopreservation. Fig. 4 reveals the changes in sperm motility of twenty patients after 90 min incubation in vials without and with different soot patterns (the full data set, *i.e.*, the column charts at 90 min, 180 min and 270 min, along with the raw data are available as Fig. S1–S3† and Table S1 in ESI†).

The plotted columns divulge very interesting trends from a medical point-of-view, namely, the number of patients whose ejaculates contain \sim 50–70% progressively motile spermatozoa (*i.e.*, normozoospermia) is twice as large after the addition of *soot3* compared to the control (see Fig. 4a). Also, there is an equal number of seminal fluids characterized by more than 50% immotile gametes, class *d*, if collating the same probes (eight patients from the control and *soot3* vials have $d \geq 50\%$), but the severe asthenozoospermia ($d \geq 70\%$) is remarkably declined due to the presence of soot (see Fig. 4c). Such experimental results hint at favorable impact of the soot rather than cytotoxicity if concerning the sperm motility, which is verified by the statistical analysis of the raw data, shown in Fig. 5.

The mean values of data populations reaffirm the effects discussed above and on an average basis, the specimens mixed with *soot1* and *soot3* seem to activate the non-progressive and immotile species, transforming them into progressively motile spermatozoa. Moreover, the standard deviation is relatively constant for the different data sets (see Fig. 5), meaning that the observed tendencies originate from real biophysical/biochemical phenomena at the seminal fluid-soot-sperm cell contact interface rather than a measurement error.

Intriguingly, the sperm activation diminishes in the middle incubation period around 180 min (see Fig. 5 and Fig. S2 in

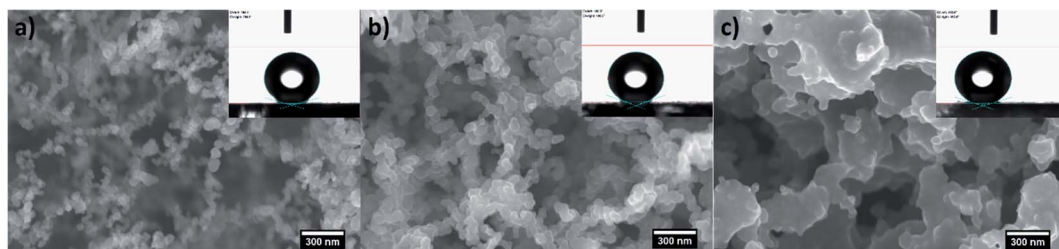


Fig. 1 Structure and morphology of the soot formed at air flow values of (a) $0.0052 \text{ m}^3 \text{ min}^{-1}$ – *soot1*, (b) $0.0042 \text{ m}^3 \text{ min}^{-1}$ – *soot2* and (c) $0.0033 \text{ m}^3 \text{ min}^{-1}$ – *soot3*. The insets illustrate the static contact angle of $10 \mu\text{L}$ water droplets attached to the soot-coated surfaces.



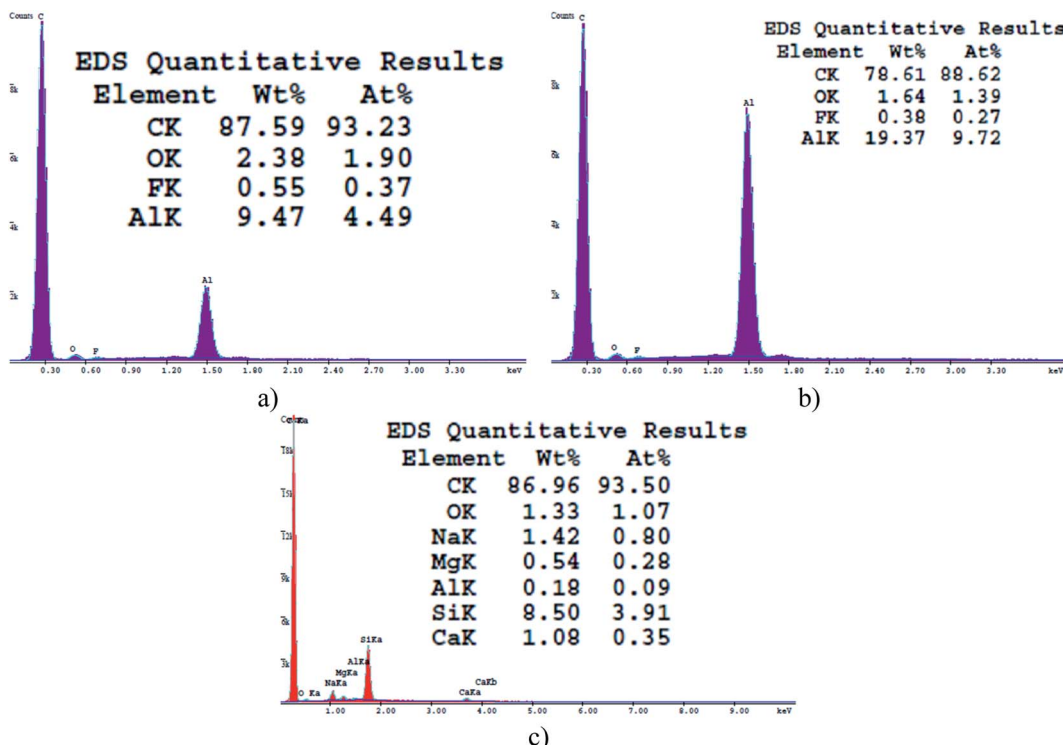


Fig. 2 EDS spectra of the soot formed at air flow values of (a) $0.0052 \text{ m}^3 \text{ min}^{-1}$ – soot1, (b) $0.0042 \text{ m}^3 \text{ min}^{-1}$ – soot2 and (c) $0.0033 \text{ m}^3 \text{ min}^{-1}$ – soot3. The appearance of elements such as Na, Mg, F, Si, etc. is attributed to the chemical composition of the Biosigma VBS655/A glass slides.

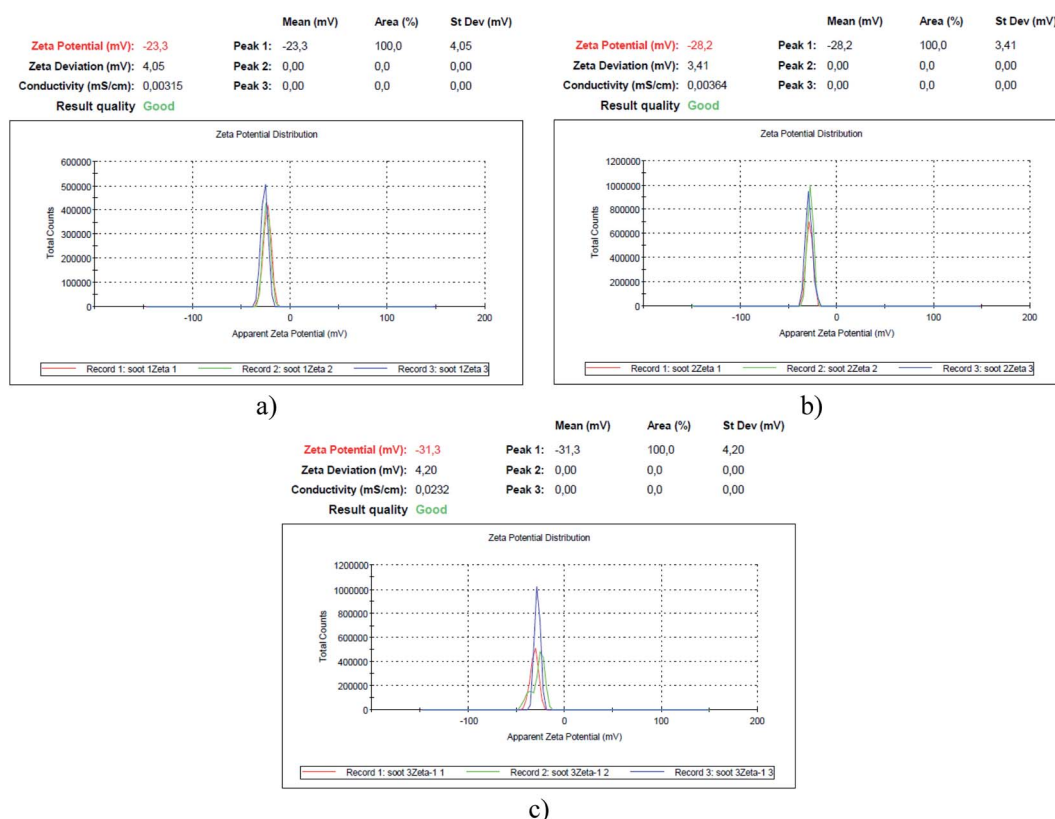


Fig. 3 Zeta potential of the soot formed at air flow values of (a) $0.0052 \text{ m}^3 \text{ min}^{-1}$ – soot1, (b) $0.0042 \text{ m}^3 \text{ min}^{-1}$ – soot2 and (c) $0.0033 \text{ m}^3 \text{ min}^{-1}$ – soot3.

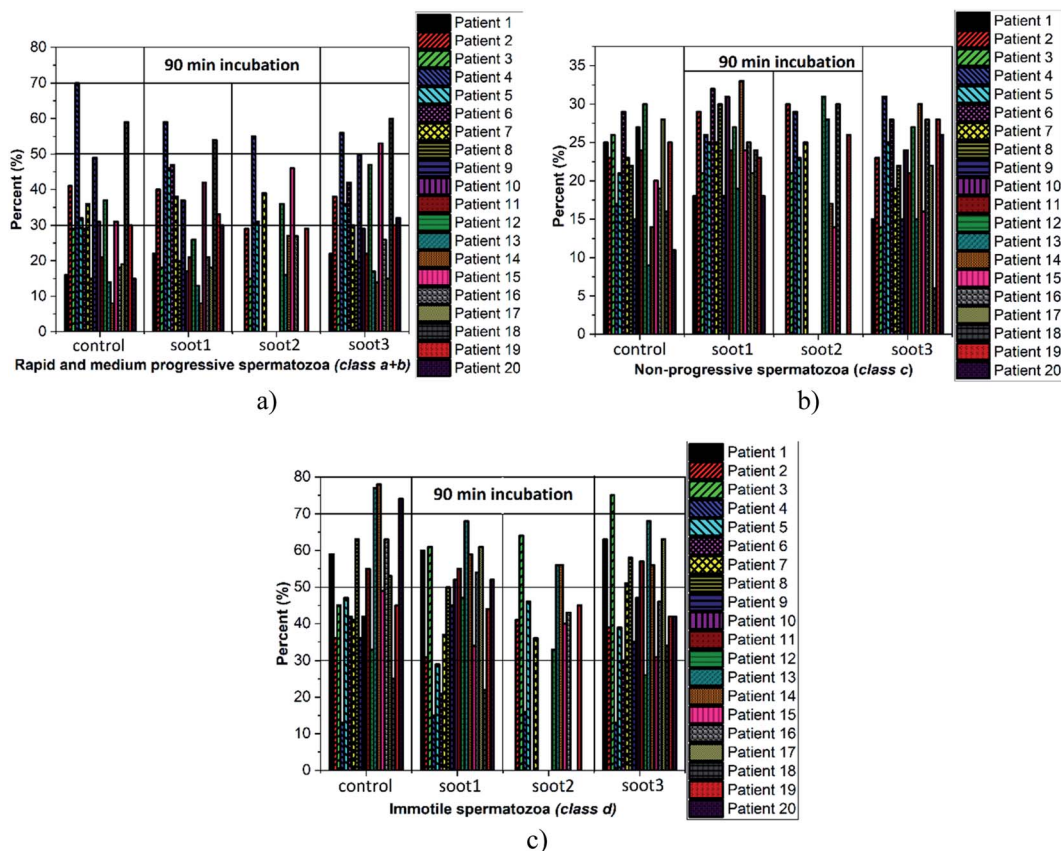


Fig. 4 Percentage of (a) progressively motile, (b) non-progressively motile and (c) immotile spermatozoa at twenty patients after 90 min residence in vials without (control) and with soot1, soot2 and soot3. The column charts symbolize an integer of the progressively motile, non-progressively motile and immotile species, detected in each human ejaculate by the Sperm Class Analyzer software, whose measurement uncertainty is $\sim 1\%$.

ESI[†]) and in fact, worsening in the progressive motility is registered at 80–85% of patients, as summarized in Table 1. Likely, the exhaustion of nutritive ingredients in the seminal plasma aggravates the semen parameters⁴⁹ but the highest soot-triggered motility reduction does not exceed 19% (see the numerical data for *patients 4 and 10* in Table S1 in ESI[†]). At the end of the incubation period, while all of the control

suspensions consist of spermatozoa class $a + b \leq 30\%$, the spherical and quasquare-shaped soot aggregates (*i.e.*, soot1 and soot3) “regenerate” a fraction of the sperm cells and enhance their motility, as noticed at 1–2 out of 15 tested subjects (see Fig. S3 in ESI[†]). The number of patients is reduced at that stage because five individuals possessed severely deteriorated seminal parameters ($d \geq 90\%$) of the control sample).

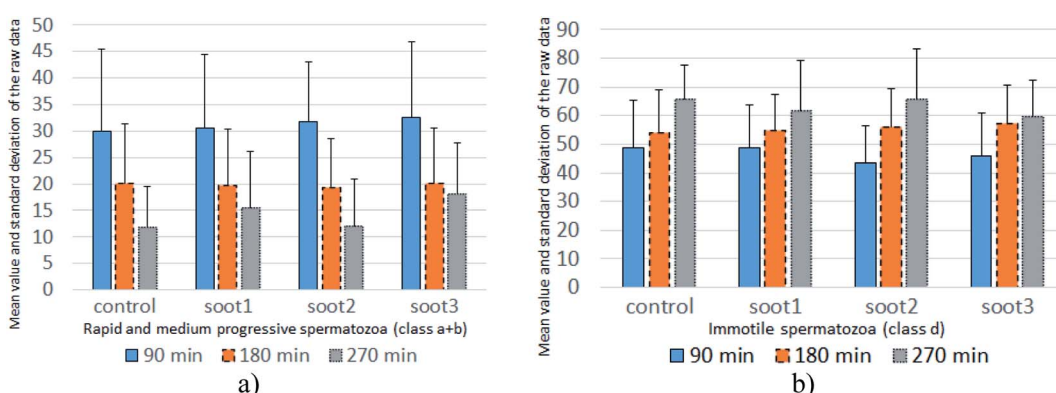


Fig. 5 Mean value and standard deviation of the raw data accounting for the percentage of (a) progressively motile and (b) immotile spermatozoa at twenty patients.

Table 1 Percentage of tested patients with progressively motile (class $a + b$) and immotile (class d) spermatozoa in the range of 30–50–70% after 270 min incubation in vials without (control – C) and with different types of rapeseed oil soot (S1 – soot1; S2 – soot2; S3 – soot3). The threshold values reflect the transitions between two diametrically opposed medical conditions such as normozoospermia and asthenozoospermia

Motility class (%)	Percentage of tested patients falling into a certain motility range											
	90 min			180 min			270 min					
	C	S1	S2	S3	C	S1	S2	S3	C	S1	S2	S3
$a + b \geq 50$	10	10	9	20	0	0	0	0	0	0	0	0
$30 \leq a + b \leq 50$	35	40	36	35	20	20	18	15	0	13	0	7
$a + b \leq 30$	55	50	55	45	80	80	82	85	100	87	100	93
$d \leq 50$	60	55	73	60	40	35	18	25	7	20	33	33
$50 \leq d \leq 70$	25	45	27	35	50	55	73	60	60	53	33	47
$d \geq 70$	15	0	0	5	10	10	9	15	33	27	33	20

Albeit informative, Table 1 does not generalize the appearance of fluctuations in the semen quality at patients with reproductive problems, *i.e.*, whose gametes fall within $a + b \leq 30\%$ or $d \geq 70\%$. For example, the progressively motile spermatozoa at *patient 1* increase from 16% to 22% upon 90 min incubation with *soot1* or *soot3* in spite of the asthenozoospermia (see Fig. 4a). Thus, such important motility changes must be carefully addressed in Fig. 6 with the aim of showing to what extent the different soot powders exhibit activation, neutral or cytotoxic properties.

As seen, the rapeseed oil soot is basically non-cytotoxic or in the worst-case scenario mildly toxic, since collapse in the progressive sperm motility is identified at not more than 20% of tested individuals around 270 min incubation (see Fig. 6a and Table S1 in ESI†). In comparison, about 93% of all control seminal suspensions at that time are with inherently reduced quality, clearly demonstrating the advantage of inserting soot in the fresh ejaculates. Meanwhile, the soot-governed

activation effects against the progressively motile and immotile spermatozoa encompass ~50–60% and ~33–65% of all patients, respectively (see Fig. 6, 270 min), confirming the harmless use of this material in cryobiology³² and opening opportunities for its future integration in reproductive medicine as an effective tool for functional stimulation of fresh and thawed human semen.

3.3. Insights into the soot–spermatozoa interaction mechanisms

The large surface-to-volume ratio and functional properties of many nanoparticles (*e.g.*, silver, cerium oxide, magnesium oxide, zinc oxide) imply a potential hazard, since the eukaryotic sperm cells may internalize them by endocytosis (absorption of external material by engulfing it within the cell membrane).⁴⁴ In turn, the penetration of oppositely charged nanoparticles may violate the membrane-associated energetic function and intoxicate the living cell to an extent depending on the particle size (the smaller the particles, the higher their nanotoxicity).^{44,45} Focusing on the toxicological mechanisms of soot aerosols, their high surface oxidation and hydrophilicity facilitate the generation of reactive oxygen species (ROS), promoting morphological and chemical contact with hydrophilic biomolecules produced by the human lung cells, peripheral blood monocyte-derived macrophage cells or A549-type cells.^{50–57} This is accompanied by cell swelling and membrane blebbing,⁵⁰ phagocytosis⁵¹ or cytoplasm internalization of soot,⁵⁵ where the smaller nanoparticles⁵¹ and those with increased concentration of environmentally persistent free radicals (EPFR) exhibit the highest nanotoxicity.⁵⁵

Nevertheless, the non- or mild cytotoxicity of the rapeseed oil soot (at one order of magnitude higher concentration compared to stove-released soot⁵⁵) has its scientific explanation: if appears as a functional coating, the soot is superhydrophobic and when peeled off, it is still extremely water-repellent and does not mix well with watery liquids (*e.g.*, seminal fluids) for at least 90 min, as demonstrated in Fig. 7.

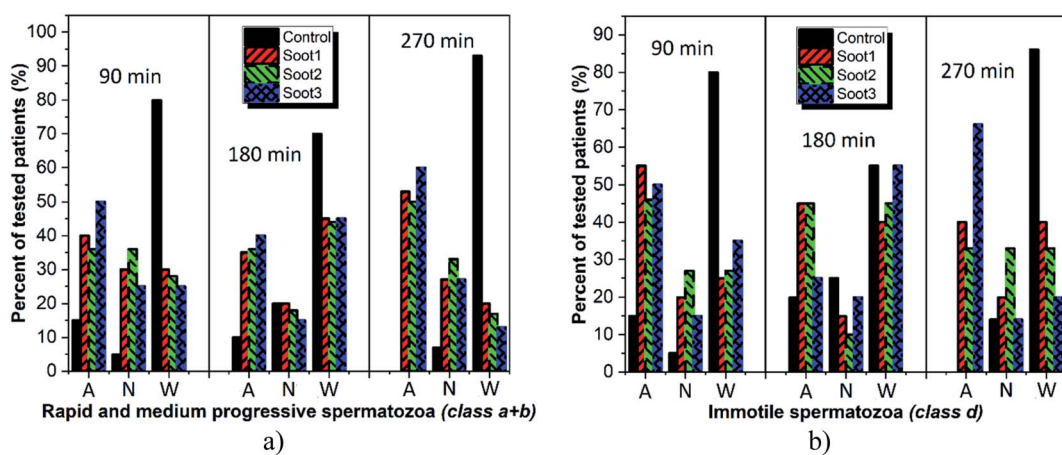


Fig. 6 Activation (A), neutral (N) and cytotoxic (W) effects of the soot nanoparticles towards (a) progressively motile and (b) immotile human spermatozoa within 270 min incubation period. The column charts symbolize the percentage of tested patients at which are observed the particular effects (e.g., A = 60%–270 min, means that in 9 out of 15 patients is registered sperm motility activation).



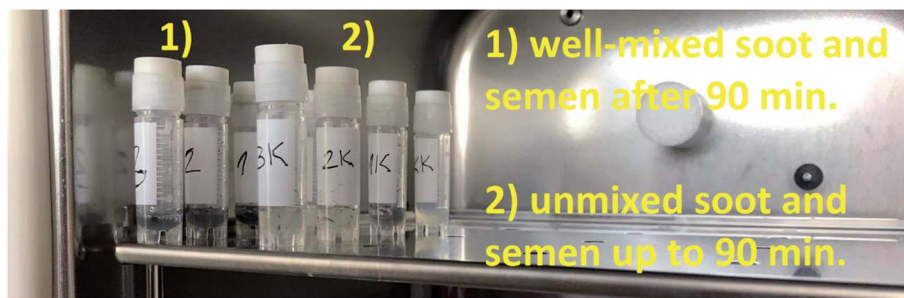


Fig. 7 A photograph of soot nanoparticles in human seminal fluids.

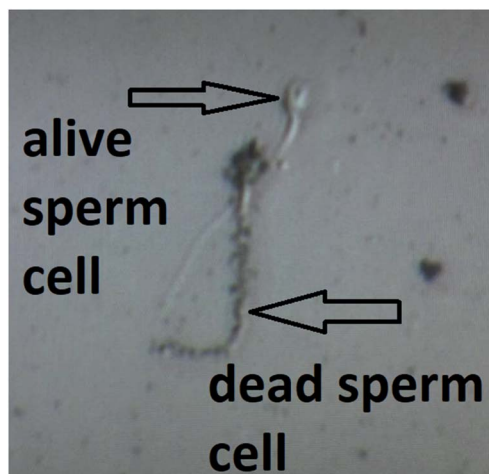


Fig. 8 A high-resolution optical image of live and dead human spermatozoa in a soot-seminal suspension.

This features of the soot nanoparticles and their weak surface oxidation ($\sim 1.1\text{--}1.9$ at%) imply predominantly physical (electrostatic) interactions with the gametes and lower concentrations of ROS compared to the diesel soot,⁵¹ which ceases the endocytosis. Even upon prolonged incubation (e.g., 180 min), part of the hydrophobic soot remains in the form of large carbon agglomerates (see the left-hand side of Fig. 7) hampering the cell internalization, identically to the soot emitted from old diesel engines.⁵¹ Lastly, the negatively charged soot (see Fig. 3) electrostatically repels the human spermatozoa, whose zeta potential is also negative,⁴³ and thereby, the lack of continuous contact prevents the membrane penetration and cell intoxication. Such a statement is validated by a high-resolution optical microscope image, labelled as Fig. 8,

showing that a live sperm cell successfully hinders the adherence of soot to its head, body and tail, probably due to electrostatic repulsions, contrary to a dead spermatozoon entirely coated with carbon nanoparticles. To the best of our knowledge, this is the first scientific discovery of the aforesaid phenomenon, having strong potential for being elaborated into a unique method for the selection of viable spermatozoa from native ejaculates and testicular biopsies in an effort of improving the outcome of *in vitro* fertilization (IVF) and mitigating the male factor infertility.⁵⁸

Mentioning the occurrence of electrostatic forces in the soot-enriched semen, we hypothesize that they are primarily accountable for the sperm motility activation reported in the majority of patients (as a proof-of-concept, see Videos S1 and S2 in ESI†). The soot nanoparticles form an electrostatic field around the negatively charged gametes and transfer momentum and kinetic energy (equivalently to the elastic collisions of gas molecules), accelerating their motion (see Videos S3 and S4 in ESI†). The acquired physical impulse “embitters” the spermatozoa and they start disintegrating and reshaping the carbon clusters by implicating the neighboring sperm cells in a chain reaction, as suggested by the images in Fig. 9.

Our assumptions are in compliance with the zeta potential values of the studied soot patterns and the most negatively charged *soot3* has the best activation ability toward progressively motile human gametes (class *a + b*), including 40–60% of all patients throughout the incubation period (see Fig. 6a).

3.4. Remaining challenges to “real-life” medical applications

The nanotechnology discussed herein is in a final phase in terms of its clinical integrability, as long as the synthesis of

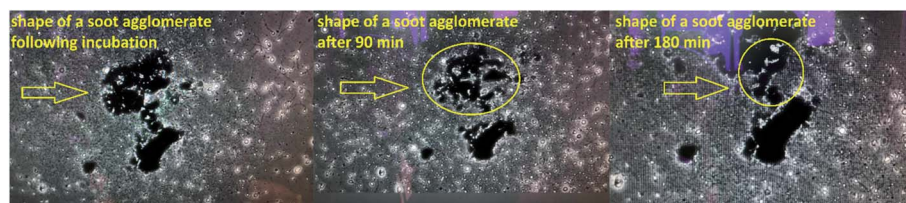


Fig. 9 Sperm-driven disintegration and reshaping of a soot agglomerate.



rapeseed oil soot nanoparticles and their dispersion in vials is not time-consuming and does not require specialized equipment or multiple and expensive chemicals, *i.e.*, it can be implemented immediately at low cost (literally pennies). Notwithstanding, a few challenges remain to be addressed *via* the next mandatory research steps preceding the commercialization. At first place, while quite credible, the hypotheses for electrostatic activation do not explain why the specific soot acts either a motility accelerator or decelerator, depending on the patient. We believe that the biochemical composition of the semen plays a role in the reaction mechanisms and likely the soot absorbs harmful constituents from the seminal plasma (*e.g.*, the prostatic fraction that is more detrimental to the long-term preservation of sperm motility⁵⁹), which is possible if taking into account the soot interactions with some urine compounds available in the human ejaculate too.⁶⁰ Therefore, detailed biochemical characterization of a set of native ejaculates before and after the addition of soot must be performed, along with assessing its nanotoxicity in the absence of a seminal plasma (to be able to separate the electrostatic effects from those induced by the plasma). Besides, the secretion of oxygen free radicals is detrimental to the sperm cells⁶¹ and a future important study will examine the ROS production by the distinct rapeseed oil soot patterns, facilitating the better understanding of the soot's protective functions. Finally, it needs to be clarified whether the soot induces acrosome reactions or hyperactivation since these are pivotal stages in reproductive biology. In cases of intracytoplasmic sperm injection (ICSI), where an immobilized sperm cell is injected *via* a needle in the ovum's interior, any acrosome reactions provoked by the soot will benefit the cell's functional maturity and its capability of fertilizing the female gamete. If the soot treatments instigate hyperactivation (enhancement of the vibration amplitude of spermatozoon's flagellum, promoting easier penetration through the ovum's zona pellucida), our method would be more appropriate for classical *in vitro* or insemination, where the processed spermatozoa are placed in a little drop of culture media or the woman's uterus using a catheter, respectively, and the male gametes alone can initiate acrosome reaction and subsequent natural fertilization of the oocyte. These tasks cannot be delivered within a single article and thus are planned as upcoming systematic experiments, as part of a research project no. KP-06-H57/1.

4. Conclusions

The prolonged residence of spherical, incompletely merged or fused rapeseed oil-derived soot in native human seminal fluids with divergent parameters (sperm concentration and motility) ended up without identifying serious degradation in the percentage of motile spermatozoa juxtaposed to the control suspensions (maximum reduction of progressive motility by 19%). Surprisingly, all types of soot nanoparticles/aggregates, more or less, served as functional activators and at ~40–60% of tested men, the immotile and/or non-progressive gametes were transformed into motile species. Electrostatic soot-semen repulsive forces were found to transfer motional energy to the

sperm cells and enhance their motility, which in turn led to rearrangement of the original soot agglomerates. The obtained results inferred also that any soot-triggered variations in the biochemistry of human semen from patient-to-patient might be a complementary mechanism provoking the speeding up/slowing down effects, which is an assertion that needs to be studied further. The as-synthesized soot demonstrated the aptitude for future replacement of the commercially available phosphodiesterase inhibitors (*e.g.*, pentoxifylline) improving the sperm's functional competence prior to IVF procedures, but at the expense of premature acrosome reactions or toxicity towards the oocyte function and early embryo development.⁶²

Patents

A Bulgarian patent application (No. 113453) was submitted on November 30th 2021 as a result of the work reported herein.

Author contributions

Dr Esmeryan and Mr Chaushev conceived the idea to study the degree of cytotoxicity of three types of hydrophobic carbon soot towards human spermatozoa. They planned, designed and implemented the experiments, except the surface characterization. Dr Esmeryan processed and interpreted the data, performed the statistical analysis and data sorting, proposed the fundamental aspects of soot-spermatozoa interactions, contrived the scientific concept of the article and wrote its first and final versions. Mr Rangelov actively participated in the execution of experiments and the data acquisition. All authors approved the scientific content of the manuscript prior to submission.

Conflicts of interest

The authors declare that they have not known competing financial interests or personal relationships that could have appeared to influence the work reported in this paper.

Acknowledgements

This research was performed thanks to the financial support of Bulgarian National Science Fund under grant no. KP-06-H57/1/15.11.2021. The authors wish to sincerely acknowledge prof. Tsvetanka Babeva (Director of IOMT-BAS) and Dr Petia Petrova ("Optical transducers" Laboratory, IOMT-BAS) for kindly organizing and implementing the zeta potential analysis. Dr Esmeryan acknowledges Dr Reza Mohammadi and Dr Carlos Castano (VCU-USA) for providing the high-resolution SEM images and the EDS spectra.

References

- 1 J. C. Lucke and W. Hall, *EMBO Rep.*, 2005, **6**, 98–102.
- 2 T. H. Jang, S. C. Park, J. H. Yang, J. Y. Kim, J. H. Seok, U. S. Park, C. W. Choi, S. R. Lee and J. Han, *Integr. Med. Res.*, 2017, **6**, 12–18.



3 H. Devlin, *The Cryonics Dilemma: Will Deep-Frozen Bodies Be Fit for New Life?*, The Guardian, 2016, <https://www.theguardian.com/science/2016/nov/18/the-cryonics-dilemma-will-deep-frozen-bodies-be-fit-for-new-life>; last accessed: November 30th 2021.

4 H. Breithaupt, *EMBO Rep.*, 2012, **13**, 394.

5 F. Lotti and M. Maggi, *Nat. Rev. Urol.*, 2018, **15**, 287–307.

6 A. Sansone, C. D. Dato, C. de Angelis, D. Menafra, C. Pozza, R. Pivonello, A. Isidori and D. Gianfrilli, *Reprod. Biol. Endocrinol.*, 2013, **16**, 3.

7 C. Krausz and A. Riera-Escamilla, *Nat. Rev. Urol.*, 2018, **15**, 369–384.

8 C. Barratt, *Most Men in the US and Europe Could Be Infertile by 2060, According to a New Study*, Quartz, 2021, <https://qz.com/1040302/most-men-in-the-us-and-europe-could-be-infertile-by-2060-according-to-a-new-study/>, last accessed: November 30th.

9 H. Bai, Y. Zhang, S. Tian, R. Hu, Y. Liang, J. Gao, Y. Wang and B. Wu, *Cryobiology*, 2020, **95**, 138–142.

10 J. Liu, C. Tanrikut, D. L. Wright, G. Y. Lee, M. Toner, J. D. Biggers and T. L. Toth, *Cryobiology*, 2016, **73**, 162–167.

11 C. G. Dearing, C. N. Jayasena and K. S. Lindsay, *Cryobiology*, 2017, **79**, 9–13.

12 M. Hezavehei, M. Sharifi, H. M. Kouchesfahani, R. Henkel, A. Agrawal, V. Esmaeili and A. Shahverdi, *Reprod. Biomed. Online*, 2018, **37**, 327–339.

13 J. Valipour, M. S. Nashtaei, Z. Khosravizadeh, F. Mahdavinezgad, S. Nekoonam, S. Esfandyari and F. Amidi, *Cryobiology*, 2021, **99**, 122–130.

14 C. Herbemont, S. Mnallah, B. Bennani-Smires, M. Peigne, I. Cedrin-Durnerin, M. Grynberg and C. Sifer, *Cryobiology*, 2021, **99**, 103–105.

15 F. Safian, M. G. Novin, H. Nazarian, Z. S. Mofarahe, M.-A. Abdollahifar, V. Jajarmi, S. Karimi, M. Kazemi, S. Chien and M. Bayat, *Cryobiology*, 2021, **98**, 239–244.

16 S. I. Moskovtsev, A. G.-M. Lulat and C. L. Librach, Cryopreservation of human spermatozoa by vitrification vs. slow freezing: Canadian Experience, in, *Current Frontiers in Cryobiology*, ed., Igor I. Katkov, Intech Open, Chapter 3, 2012, pp. 77–101.

17 M. Di Santo, N. Tarozzi, M. Nadalini and A. Borini, *Adv. Urol.*, 2012, **2012**, 854837.

18 D. E. Pegg, *Cryobiology*, 2020, **93**, 3–11.

19 G. J. Morris, E. Acton, B. J. Murray and F. Fonseca, *Cryobiology*, 2012, **64**, 71–80.

20 Y. Tao, E. Sanger, A. Saewu and M.-C. Leveille, *Reprod. Biol. Endocrinol.*, 2020, **18**, 17.

21 F. Franks, *Cryobiology*, 1983, **20**, 335–345.

22 S. Bhattacharya and B. G. Prajapati, *Asian J. Pharm.*, 2016, **10**, 154–159.

23 B. P. Best, *Rejuvenation Res.*, 2015, **18**, 422–436.

24 S.-J. Yoon, M. S. Rahman, W.-S. Kwon, Y.-J. Park and M.-G. Pang, *PLoS ONE*, 2016, **11**, e0152690.

25 M. Wang, P. Todorov, E. Isachenko, G. Rahimi, W. Wang, M. von Brandenstein, P. Kumar, P. Mallmann and V. Isachenko, *Cryobiology*, 2021, **99**, 95–102.

26 A. Agha-Rahimi, M. A. Khalili, S. A. Nottola, S. Miglietta and A. Moradi, *Andrology*, 2016, **4**, 1037–1044.

27 M. Petrushko, T. Yurchuk, P. Todorov, E. Hristova, V. Piniaiev, E. Isachenko, G. Rahimi, P. Mallmann and V. Isachenko, *Cryobiology*, 2021, **103**, 39–44.

28 N. J. Shirtcliffe, G. McHale, S. Atherton and M. I. Newton, *Adv. Colloid Interface Sci.*, 2010, **161**, 124–138.

29 A. Alizadeh, M. Yamada, R. Li, W. Shang and S. Otta, *et.al.*, *Langmuir*, 2012, **28**, 3180–3186.

30 L. B. Boinovich, A. M. Emelyanenko, V. V. Korolev and A. S. Pashinin, *Langmuir*, 2014, **30**, 1659–1668.

31 X. Wu, V. V. Silberschmidt, Z.-T. Hu and Z. Chen, *Surf. Coat. Technol.*, 2019, **358**, 207–214.

32 K. D. Esmeryan, Y. Lazarov, G. S. Stamenov and T. A. Chaushev, *Cryobiology*, 2020, **92**, 263–266.

33 J. Saragusty and A. Arav, *Reproduction*, 2011, **141**, 1–19.

34 K. D. Esmeryan, C. E. Castano, S. D. Gyohev, Y. Lazarov, N. I. Stoimenov and R. Mohammadi, *Curr. Appl. Phys.*, 2021, **31**, 74–86.

35 T. Jeyaseelan, P. Ekambaram, J. Subramanian and T. Shamim, *Renewable Sustainable Energy Rev.*, 2022, **157**, 112073.

36 I. C. Jaramillo, A. Sturrock, H. Ghiassi, D. J. Woller, C. E. Deering-Rice, J. S. Lighty, R. Paine, C. Reilly and K. E. Kelly, *J. Environ. Sci. Health, Part A: Toxic/Hazard. Subst. Environ. Eng.*, 2018, **53**, 295–309.

37 K. D. Esmeryan, C. E. Castano, A. H. Bressler, C. P. Fergusson and R. Mohammadi, *RSC Adv.*, 2016, **6**, 61620–61629.

38 K. D. Esmeryan, C. E. Castano, R. Mohammadi, Y. Lazarov and E. I. Radeva, *J. Phys. D: Appl. Phys.*, 2018, **51**, 055302.

39 K. D. Esmeryan, S. D. Gyohev, C. E. Castano and R. Mohammadi, *J. Phys. D: Appl. Phys.*, 2021, **54**, 015303.

40 K. D. Esmeryan, C. E. Castano, A. H. Bressler, M. Abolghasemibizaki, C. P. Fergusson, A. Roberts and R. Mohammadi, *Diamond Relat. Mater.*, 2017, **75**, 58–68.

41 N. R. Geraldi, L. E. Dodd, B. B. Xu, D. Wood, G. G. Wells, G. McHale and M. I. Newton, *Bioinspiration Biomimetics*, 2018, **13**, 024001.

42 K. D. Esmeryan, C. E. Castano, Y. I. Fedchenko, R. Mohammadi, I. K. Miloushev and K. A. Temelkov, *Colloids Surf. A*, 2019, **567**, 325–333.

43 M. Ionov, W. Gontarek and M. Bryszewska, *MethodsX*, 2020, **7**, 100895.

44 H. Schwegmann, A. J. Feitz and F. H. Frimmel, *J. Colloid Interface Sci.*, 2010, **347**, 43–48.

45 D. G. Deryabin, L. V. Efremova, A. S. Vasilchenko, E. V. Saidakova, E. A. Sizova, P. A. Troshin, A. V. Zhilenkov and E. A. Khakina, *J. Bionanotechnol.*, 2015, **13**, 50.

46 H. Huang, X. Zhang, X. Xiao and S. Ye, *Sci. Prog.*, 2020, **103**, 1–12.

47 K. Suttiponparnit, J. Jiang, M. Sahu, S. Suvachittanont, T. Charinpanitkul and P. Biswas, *Nanoscale Res. Lett.*, 2021, **6**, 27.

48 J. P. Holmberg, E. Ahlberg, J. Bergenholz, M. Hassellöv and Z. Abbas, *J. Colloid Interface Sci.*, 2013, **407**, 168–176.

49 A. Makler, I. Zaidise, E. Paldi and J. M. Brandes, *Fertil. Steril.*, 1979, **31**, 147–154.



50 W. J. Catallo, C. H. Kennedy, W. Henk, S. A. Barker, S. C. Grace and A. Penn, *Environ. Health Perspect.*, 2001, **109**, 965–971.

51 D. S. Su, A. Serafino, J. O. Müller, R. E. Jentoft, R. Schlögl and S. Fiorito, *Environ. Sci. Technol.*, 2008, **42**, 1761–1765.

52 A. E. Holder, B. J. Carter, R. G. Goldstein, D. Lucas and C. P. Koshland, *Atmos. Pollut. Res.*, 2012, **3**, 25–31.

53 M. Antinolo, M. D. Willis, S. Zhou and J. P. D. Abbott, *Nat. Commun.*, 2015, **6**, 6812.

54 R. Niranjan and A. K. Thakur, *Front. Immunol.*, 2017, **8**, 763.

55 H. Jia, S. Li, L. Wu, S. Li, V. K. Sharma and B. Yan, *Environ. Sci. Technol.*, 2020, **54**, 5608–5618.

56 Z. H. Zhang, E. Hartner, B. Uttinger, B. Gfeller, A. Paul, M. Sklorz and H. Czech, *et.al.*, *Atmos. Chem. Phys.*, 2022, **22**, 1793–1809.

57 Y. T.-H. Le, J.-S. Youn, H.-G. Moon, X.-Y. Chen, D.-I. Kim, H.-W. Cho, K.-H. Lee and K.-J. Jeon, *Nanomaterials*, 2021, **11**, 1455.

58 V. Mangoli, R. Mangoli, S. Dandekar, K. Suri and S. Desai, *Fertil. Steril.*, 2011, **95**, 631–634.

59 S. Sanada, E. Arai, M. Ueda, K. Ogura and O. Yoshida, *Acta Urol. Jpn.*, 1988, **34**, 1965–1972.

60 K. D. Esmeryan and T. A. Chaushev, *Sens. Actuators, A*, 2021, **317**, 112480.

61 A. Agarwal, G. Virk, C. Ong and S. S. du Plessis, *World J. Men's Health*, 2014, **32**, 1–17.

62 M. Satish, S. Kumari, W. Deeksha, S. Abhishek, K. Nitin, S. K. Adiga, P. Hegde, J. P. Dasappa, G. Kalthur and E. Rajakumara, *Sci. Rep.*, 2021, **11**, 12293.

